A Loarte et al.

Evolution of plasma parameters in the termination phase of high confinement H-modes at JET and implications for ITER

Evolution of Plasma Parameters in the Termination Phase of High Confinement H-modes at JET and Implications for ITER

A. Loarte[1], F. Koechl[2], M.J. Leyland[3], A. Polevoi[1], M. Beurskens[4], V. Parail[5], I. Nunes[6], G.R. Saibene[7], R.I.A. Sartori[7] and JET EFDA contributors*

JET-EFDA, Culham Science Centre, OX14 3DB, Abingdon, UK

[1]*ITER Organization, Route de Vinon sur Verdon, 13115 Saint Paul Lez Durance, France*
[2]*Association EURATOM-ÖAW/ATI, TU Wien, Atominstitut, 1020 Vienna, Austria*
[3]*York Plasma Institute, Department of Physics, University of York, Heslington, York, YO10 5DD, UK*
[4]*Max-Planck-Institut für Plasmaphysik, EURATOM Association, 85748 Garching, Germany*
[5]*EURATOM-CCFE Fusion Association, Culham Science Centre, OX14 3DB, Abingdon, OXON, UK*
[6]*Centro de Fusao Nuclear, Associação EURATOM-IST, Lisboa, Portugal*
[7]*Fusion for Energy, C/ Josep Pla nº 2, 08019 Barcelona, Spain*
* See annex of F. Romanelli et al, "Overview of JET Results",
(24th IAEA Fusion Energy Conference, San Diego, USA (2012)).

ABSTRACT

The evolution of the plasma parameters in the termination phase of high confinement H-modes at JET with CFC plasma facing components (JET-C) has been analyzed with a view to predict the dynamics of the plasma energy decrease for sudden terminations of the ITER Q_{DT} =10 scenario caused by malfunction of additional heating systems. JET-C experiments show that the rate of decay of the plasma energy in the high performance H-mode termination phase is predominantly determined by the duration of the Type III ELMy H-mode phase after the end of the Type I ELMy H-mode regime. Longer Type III ELMy H-mode phase durations lead to slower plasma energy decay rates. The duration of the Type III ELMy H-mode phase is itself determined by the margin of the edge power flow (dominated by the rate of collapse of the plasma energy) over the H-mode threshold power in the termination phase, with larger margins leading to longer Type III ELMy H-mode phase durations. For most of the JET-C discharges analyzed the timescale for the plasma energy decrease in the termination of high energy confinement H-modes is comparable to the energy confinement time of the plasma in the high confinement phase rather than half of this value, which is to be expected for instantaneous H-L transitions. Modelling of the termination phase of ITER Q_{DT} =10 H-modes (with transport assumptions in this phase validated against JET-C experiments) shows that similar to JET-C results the timescale for the decrease of the plasma energy is comparable and can even be longer than the energy confinement time of the burning phase, provided that ELM control can be maintained. This is due to the long sustainment of the Type III ELMy H-mode mode by the substantial edge power flow compared to the H-mode threshold power during this phase. The large edge power flow in the termination phase of ITER high Q_{DT} plasmas is provided by the decrease of the plasma energy and the slow collapse of the alpha heating. Operational strategies in ITER to control the energy decay rate as well as the consequences of the lack of ELM control in the high Q_{DT} termination phase are presented.

1. INTRODUCTION

Plasma control during energy confinement transients is expected to become more challenging for the next generation of fusion devices such as ITER. The reasons for this are twofold: one is related to the intrinsic increase of the power fluxes to plasma facing components (PFCs) during transients with increasing dimensions of the device and the other is related to the slower timescales for the reaction of the plasma position control system to changes in plasma energy compared to today's devices [9]. Sudden changes in plasma energy require a simultaneous adaptation of the vertical magnetic field applied to the plasma to control the plasma radial displacement outwards (when its energy increases) or inwards (when it decreases). These fast changes of the vertical field applied to the plasma become more challenging in next step fusion devices such as ITER because of the large inductance of the poloidal field coils (due to the machine size) and the limits on the voltage that can be applied (because they are superconducting) and the massive, double walled vacuum vessel required as main confinement barrier for Tritium and radioactive products. The vacuum vessel

is designed with a well characterized material (Stainless Steel 316L for ITER) and to withstand electromagnetic forces during disruptions. This leads to a design with thick double walls and relatively high conductivity which slows down the penetration of the vertical field applied from the PF coils (typical timescales are in the range of a second in ITER) [9].

Plasma operation in ITER high Q_{DT} scenarios foresees the controlled increase (or reduction) of the additional heating power into the plasma, which together with the concomitant increase (or reduction) of the alpha heating and the control of ELMs during these transient phases, are expected to lead to a slow reduction (or increase) of the plasma energy. Therefore the controlled access/ exit from burning plasma conditions is not expected to lead to challenges regarding the control of power fluxes to PFCs nor plasma radial position in these phases. Such ITER scenarios have been simulated in experiments at JET with the ITER-like Wall (ILW) (Be PFCs in the main chamber and a W divertor as in ITER. which we will refer to as JET-ILW) and found to be robust in terms of plasma position control and W accumulation issues [5]. However, loss of additional heating systems due to malfunction, ingress of particulates from the plasma facing components (commonly called UFOs) or lack of appropriate ELM control can potentially lead to much faster energy confinement transients in ITER [18, 28]. Large radial excursions during confinement transients in ITER diverted plasmas due to the slow reaction of the vertical field applied to the plasma can cause plasma contact with the first wall PFCs, as shown in Fig.1 for a fast transition from H mode into L-mode. This leads to deposited power fluxes well beyond their design limits [18, 24] for the worst possible cases considered. Such an event was initially modelled in [27] and shown to be avoidable either by improved plasma control [15] and operational strategies, such as increasing the gap between the plasma and wall when such transients are expected, or by performing a rapid shutdown of the plasma when a confinement transient that cannot be controlled is detected. Both of the latter options have potential operational implications for ITER either because they limit its operational space or its fusion performance (i.e. if they require a reduction of the plasma size to increase the clearance to the wall) or on its pulse repetition rate (i.e. if the plasma energy needs to be radiated during the shutdown which may require increased dwell time to pump the impurities injected).

Understanding and characterizing the plasma behaviour during these confinement transients in present experiments is required to evaluate the timescale of the plasma energy evolution during such transients in ITER and to define operational strategies to avoid excessive power fluxes on the PFCs during them. Plasma behaviour in ITER high Q_{DT} plasmas during transients is expected to be different from that in present experiments because of the dominance of the alpha heating over the additional heating power, affecting both the evolution of the plasma density and temperature during confinement transients. In turn, the evolution of the plasma density and temperature determines the magnitude of the alpha heating which also influences the plasma energy confinement regime (L-mode or H-mode of varying confinement quality) leading to a complex feedback loop. Therefore, prediction of the plasma behaviour during confinement transients in ITER cannot be done purely on empirical extrapolations from present experiments but requires modelling. Both the model and

2

the modelling assumptions applied to ITER have to be validated first against present experiments to ensure that the predictions for ITER have a firm physics basis.

From all the energy confinement transients the one which is expected to lead to the largest fluxes and the more serious plasma position control challenges in ITER is the transition from a H-mode plasma with $H_{98} = 1$ to L-mode [18, 24, 27, 28, 15]. In the $Q_{DT} = 10$ ITER reference scenario fast H-L transitions the plasma energy can potentially decrease by a factor of ~ 3 (i.e. e^{-1}) in timescales shorter than 2s [18, 28], which corresponds to the expected L-mode energy confinement time in these conditions. Transitions in which the energy confinement increases (i.e. after the L-H transition) are less challenging from the control point of view. In the L-H transitions, the expected power fluxes to PFCs are lower because the edge power flow usually decreases transiently due to the increased derivative of the plasma energy following the transition to H-mode. In addition, the timescales are long (~10s) as the plasma enters a regime with higher than L-mode energy confinement and the alpha heating in ITER requires time to build up [19, 28]. The longer timescales make the radial position of the plasma easier to control in L-H transitions than in H-L transitions.

In this paper we describe the analysis of the evolution of the plasma parameters during the sudden termination phases of a wide range of high confinement (H_{98} ~1) plasmas in the JET tokamak with a view to provide an evaluation of the plasma behaviour during the fastest energy confinement transients that can be expected in ITER. The discharges analyzed correspond to an operational period of the JET tokamak with Carbon Fibre Composite (CFC) PFCs, which we will refer to as JET-C, and span a range of plasma currents (I_p) up to 4.3MA [25]. These experiments have been selected rather than the more recent experiments in JET-ILW because the operation with CFC PFCs allowed a more abrupt termination of the additional heating to the plasma, and thus faster confinement transients, than with the more recent JET-ILW. Operation of JET-ILW makes these experiments more difficult to perform due to issues related to W accumulation and ensuing plasma disruptions [7]. The paper is organized as follows: Section 2 provides an overview of the JET-C experimental results, describes the analysis techniques used and the key results obtained for the evolution of the plasma parameters during the termination phase of high confinement H-mode plasmas at JET-C. Section 3 describes the modelling of the JET-C experimental results for selected examples with fast energy transients from which the modelling assumptions to model ITER plasmas are verified. Section 4 describes the application of the same models, with the modelling assumptions found to be suitable to describe the JET-C experiments, to ITER $Q_{DT} = 10$ plasmas in which the additional heating power is suddenly step down while ELM control is maintained during the H-mode termination phase. Section 5 provides an initial evaluation of the consequences of the loss of ELM control during this phase, in particular in relation to the main plasma behaviour in response to the W influxes into the plasma associated with the uncontrolled Type I ELMs. Finally, Section 6 summarises the results and draws conclusions.

In this paper we do not deal in detail with most of the issues associated with the longer timescale evolution (~ longer than the energy confinement time of the burning plasma) of impurities, originating

both from the W divertor and from extrinsic impurity seeding required for divertor power load and W sputtering control, during termination phase of high confinement H-mode plasmas in ITER. It is known from present experiments that insufficient degree of ELM control during the H-mode termination phase and/or insufficient power density in the central region of the plasma, together with the peaked density profiles that may transiently develop in the H-mode exit phase, can lead to impurity accumulation over long timescales. This can cause an acceleration of the H-mode collapse phase due to the increase in core radiation which can also eventually lead to the radiative collapse of the discharge [7]. The models required to evaluate this phenomenology in ITER are being presently developed and benchmarked against the experiments [1, 2] and this issue will be the topic of modelling studies for ITER in the near future.

2. EVOLUTION OF PLASMA PARAMETERS DURING THE TERMINATION PHASE OF TYPE I ELMY H-MODES AT JET-C

In order to characterise the physics processes that determine the decrease of plasma temperature and density in the termination phase of high confinement Type I ELMy H-modes, a set of JET-C H-mode discharges has been analysed. They comprise H-mode discharges with a range of plasma currents (I_p) from 1.7 MA to 4.3MA with low plasma triangularity ($\delta \sim 0.25$), dominant NBI heating and fuelling by gas puffing [25]. In these experiments the NBI heating power and the gas fuelling are switched off abruptly. Following this, the plasma transits from the Type I ELMy H-mode regime into the Type III ELMy H-mode regime with reduced pedestal plasma pressure and energy confinement and, finally, undergoes a H-L transition in which the edge transport barrier fully collapses and the plasma returns to the L-mode energy confinement regime. This typical plasma behaviour is illustrated in Fig.2 for one of these JET-C plasmas and it is typical of the experiments analyzed in this paper.

In order to characterize the time evolution of plasma parameters during this phase, measurements of the electron plasma temperature and density at two characteristic radial locations have been analyzed corresponding to $\rho = 0.2$ and 0.8, where $\rho = r/a$ is the normalized minor radius. The choice of these two particular radii is determined by diagnostic issues (the innermost measurement of the electron density and temperature profiles with the required time resolution by the High Resolution Thomson scattering in JET is $\rho = 0.2$ for these discharges) and ELM physics issues (points with $\rho > 0.8$ are strongly affected by the modulation of the ELMs at JET [17, 4]). Due to the sudden and complete switch off of the NBI heating power (which is optimum to cause the fastest possible confinement transitions) ion density and temperature measurements, which are based on active charge-exchange spectroscopy, are not available for these experiments. As shown in Fig.3, there can be sizeable delays between the collapse of the plasma density at the core and at the edge for some of these discharges leading to the transient formation of rather peaked density profiles compared to those of the stationary H-mode phase. This is illustrated in Fig.4(a) where the variation of the ratio of the edge to the core density during the H-mode termination phase is shown. The duration of this peaked density phase can be of up to 1.5s which is as long as $\sim 4 \, \tau_{E,\text{H-mode}}^{\text{flat-top}}$ for these

4

plasmas, where $\tau_{E,H\text{-mode}}^{\text{flat-top}}$ is the energy confinement time of the stationary Type I H-mode plasma preceding the termination phase. On the contrary, the electron temperature profiles show no significant change of peaking during the H-mode collapse phase and the edge and the core collapse simultaneously during this phase, as shown in Fig.4(b). The duration of the phase with peaked density profiles during the collapse of the H-mode has been characterised by analysing the ratio of the edge density ($\rho = 0.8$) to the core density ($\rho = 0.2$) and fitting it by a Gaussian in time as shown in Fig.4(a). The results of this analysis are shown in Fig.5 where the duration of the peaked density profiles is plotted versus I_p of the discharges. Contrary to a similar analysis of the density profile shape evolution in the L-H transition [18] in which hollow instead of peaked density profiles are formed, there is no clear trend of the duration of the peaked density profiles during the H-mode termination phase with I_p and there is significant scatter of this duration (a factor of ~2) even for discharges with similar I_p, as shown in Fig.5.

Following a similar approach to that in 18], the timescales for the density and temperature collapse during the Type I ELMy H-mode collapse phase have been characterized by fitting the density and temperature evolution at the two chosen representative radii in the profile (namely $\rho = 0.2$ and 0.8) by a modified hyperbolic tangent fit in time. The correspondingly equivalent exponential timescale for the collapse ($\tau_{\exp}$) is thus given by $\tau_{\exp} = \frac{1}{2} \tau_{\tanh}$, where $\tau_{\tanh}$ is the timescale for the whole evolution from Type I ELMy H-mode to L-mode, i.e. $\tau_{\tanh}$ is equivalent to the determination of the pedestal width when this scheme is applied to the analysis the spatial structure of the H-mode edge transport barrier [9]. The result of the analysis for the set of discharges considered here is shown in Fig.6(a) for the density and in Fig.6(b) for the temperature. From Figs.6(a-b) it is clear that, in general, the timescales for the decrease of the density and temperature at the edge and core of the JET-C plasmas during the Type I ELMy H-mode termination phase are usually longer than those expected from L-mode like energy confinement time scales (evaluated by assuming that $\tau_{E,L\text{-mode}} \sim \frac{1}{2} \tau_{E,H\text{-mode}}^{\text{flat-top}}$). However, there is a large scatter from discharge to discharge even for those with similar I_p, NBI heating power and gas fuelling level, etc. This in stark contrast with the results obtained for the build-up phase of the density and temperature profiles following the L-H transition at JET where the shot-to-shot variability for similar conditions was very low [19]. It should be noted that, as pointed out in [25, 19], $\tau_{E,H\text{-mode}}^{\text{flat-top}}$ is similar for all these discharges despite the large range of I_p spanned in the dataset. This is due to the fact that the plasma input power in these experiments is scaled as $P_{\text{input}} \sim I_p^{0.7} \times B_t^{0.8}$ in order to maintain a constant ratio to the level of the H-mode power threshold. The H-mode threshold is expected to scale as $P_{\text{input}} \sim <n_e>^{0.7} \times B_t^{0.8}$ [22] and $<n_e> \sim I_p$ in these JET Type I ELMy H-modes [25]. This way of increasing the input power level with I_p and B_t compensates to a large degree the increase of energy confinement time with I_p and B_t expected from the ITER H98 (y,2) scaling law [12], which is found to provide an appropriate description for the confinement level achieved in these discharges [25]. For these discharges $\tau_E \sim I_p^{0.9} \times B_t^{0.2} \times <n_e>^{0.4} \times P_{\text{input}}^{-0.7} \sim I_p^{1.3} \times B_t^{0.2} \times (I_p^{0.7} \times B_t^{0.8})^{-0.7} \sim I_p^{0.5} \times B_t^{-0.36}$, and as I_p and B_t are increased together to keep $q_{95} \sim$ constant this leads to a very weak dependence of τ_E on I_p.

Detailed analysis of the measurements during the Type I ELMy H-mode collapse phase in these experiments shows that the major source of the variability in Figs.5 and 6(a-b) is the duration of the Type III ELMy H-mode phase following the last Type I ELM in these discharges. The duration of the Type III ELMy H-mode phase shows a very large variability depending on fine details of the discharge evolution when the NBI heating is switched off, as shown in Fig. 7 for two very similar discharges. In Pulse No: 77949 the NBI switch off occurs almost simultaneously with the occurrence of a Type I ELM. Following this last Type I ELM the plasma enters a long Type III ELMy H-mode phase (of ~550ms) before the L-mode transition. On the other hand, for Pulse No: 77950 a Type I ELM occurs ~50ms before the NBI switch off, following this the plasma remains in the Type I ELMy H-mode for an additional ~200ms. After the last Type I ELM a very short Type III ELMy H-mode phase (~100ms) and the transition to L-mode follows in this case. As shown in Fig.7, the evolution of the plasma energy, core electron density and temperature after the last Type I ELM are different for both discharges and the timescale for their collapse after the last Type I ELM is faster for the discharge with the shortest Type III ELMy H-mode phase (Pulse No: 77950).

Although with some scatter, the same trend of longer Type III ELMy H-mode phases leading to a slower decrease of the plasma energy is found for all the experiments considered in this paper. Figure 8 shows the timescale for the decrease of the plasma energy after the last Type I ELM in the discharges. The timescale of the plasma energy decrease in this figure has been evaluated in two independent ways: as measured by the diamagnetic loop and by evaluating the electron total energy on the basis of the volume integral of the electron pressure measured with the High Resolution Thomson Scattering diagnostic. The experimental scatter in this figure is associated with the variability in strength of the transport barrier during the Type III ELMy H-mode phase which decreases continuously during this phase as the Type III ELMs evolve towards the L-mode transition (see Sections 3 and 4 for further details). It is important to note that, with the exception of transitions with very short Type III ELMy H-mode phases, the overall timescale for the decrease of the plasma energy in the H-mode termination phase is much longer than what would be expected for an immediate transition to L-mode (evaluated as $\tau_E^{\text{L-mode}} \sim \frac{1}{2} \tau_E^{\text{H-mode flat-top}}$). In fact, as shown in Fig. 8, the timescale for the decrease of the plasma energy in the H-mode termination phase is usually similar and can be even longer than the energy confinement time of the plasma in the high confinement H-mode stationary phase ($\tau_E^{\text{H-mode flat-top}}$).

The duration of the Type III ELMy H-mode phase itself is found to be well correlated with the magnitude of the edge power flow at the beginning of this phase of the discharge (i.e. after the last Type I ELM) with respect to the expected H-mode threshold power ($P_{\text{L-H}}$) [22], as shown in Fig.9. The edge power flow is given by :

$$P_{\text{edge}} = P_{\text{input}} - P_{\text{rad}}^{\text{bulk}} - dW_{\text{plasma}}/dt \qquad (1)$$

where P_{input} is the input power into the plasma including both additional heating and ohmic heating

($P_{input} = P_{ohmic} + P_{add}$), i.e. $P_{input} = P_{ohmic}$ at the beginning of the Type III ELMy H-mode phase in these experiments, P_{rad}^{bulk} is the radiated power in the main plasma and dW_{plasma}/dt is the derivative of the plasma energy. In these experiments the dominant term is dW_{plasma}/dt as the ohmic heating and main plasma radiated power levels are relatively small. For values of the ratio $P_{edge}/P_{L-H} \leq 1.0$ the duration of the Type III ELMy H-mode varies from being very short compared to $\tau_E^{H\text{-mode flat-top}}$ to being comparable to it, while for values of $P_{edge}/P_{L-H} \geq 1.0$ the duration of the Type III ELMy H-mode phase varies from being comparable to $\tau_E^{H\text{-mode flat-top}}$ to being up to 50% longer. This experimental finding is consistent with the lack of hysteresis on the edge power flow at which the H-L transition occurs at JET. It has been demonstrated in dedicated experiments at JET both in the JET-C and JET-ILW PFC configuration that the levels of edge power flow at which the L-H and H-L transitions occur are the same within experimental uncertainties [21]. Consistent with these detailed H-mode threshold experiments, we find that the discharges which have a larger edge power flow margin above the H-mode threshold at the beginning of the Type III ELMy H-mode phase also remain in H-mode (i.e. longer Type III ELMy H-mode phase) for a longer period. It should be noted, however, that in the detailed L-H/H-L threshold experiments in [20] the additional heating power to the plasma is reduced very slowly so that the dW_{plasma}/dt term in Eq. 1 is small and $P_{input} - P_{rad}^{bulk}$ dominates P_{edge}. In contrast, for the experiments that we analyse in this paper, the additional heating power decreases very suddenly and dW_{plasma}/dt is the dominant term of P_{edge} in Eq.1. This is one of the reasons for the experimental scatter in Figs.8 and 9, as the following feedback loop is established : a) dW_{plasma}/dt determines P_{edge} → b) P_{edge} influences whether the plasma remains in the H-mode confinement regime → c) the confinement regime of the plasma determines the subsequent decrease of the plasma energy in the absence of additional heating (i.e. dW_{plasma}/dt). The physics picture above explains very well the differences between the two discharges in Fig.7. Pulse No: 77949 undergoes the Type I → Type III ELMy H-mode transition at higher plasma energy than Pulse No: 77950 (which has remained for ~ 200m s in the Type I ELMy H-mode phase with ohmic heating alone). This leads to a larger ratio of P_{edge}/P_{L-H} after the last Type I ELM which helps the plasma remaining in the Type III ELMy H-mode transition for a longer period for Pulse No's: 77949 than for 77950.

3. MODELLING OF EVOLUTION PLASMA PARAMETERS DURING THE TERMINATION PHASE OF TYPE I ELMY H-MODES AT JET

Evaluating the plasma behaviour during the termination phase of high Q_{DT} plasmas in ITER requires modelling and the models applied have to be validated against experiment. Modelling of the termination of JET-C H-mode plasmas has been previously carried out by JINTRAC [3]. The Type I ELMy H-mode phase is modelled by applying a reduction of energy and particle transport to the pedestal region, which is itself limited by an MHD-like pressure limit, and an H-mode like transport model for the energy and particle transport in the core plasma such as Bohm-gyroBohm tuned to reproduce GLF23 (we will call it BgB-H-mode) or GLF23 itself [26]. During the termination phase,

while the plasma remains in the Type III ELMy H-mode, the core plasma transport is assumed to be described by an H-mode like transport model (GLF23 or BgB-H-mode) while the pedestal transport remains much lower than expectations for turbulent L-mode transport in this region but not as low as the levels required to model the edge pedestal in the Type I ELMy H-mode [3]. After the plasma undergoes the H-L transition the pedestal plasma transport reduction is removed and an L-mode like transport model for the main plasma (including the pedestal region) is applied, such as Bohm-GyroBohm, which reproduces very well JET L-mode transport (we will call it BgB-L-mode) [8]. To determine whether this general modelling approach applies to the particular JET-C experiments analyzed in this paper, we have verified it independently by performing ASTRA modelling with BgB-H-mode (and a reduction of transport at the edge transport barrier for H-mode) and BgB-L-mode (for the L-mode phase) models for two pairs of JET-C discharges. They correspond to discharges with short and long Type III ELMy H-mode transitions at two different plasma currents in these series of experiments. As shown in Fig.10, it is indeed found that for the modelling of discharges with short Type III ELMy H-mode phases, the transition from Type I ELMy H-mode to L-mode requires both a sudden disappearance of the pedestal transport barrier and a change of main plasma transport model from BgB-H-mode to BgB-L-mode. Otherwise it is not possible to correctly model the behaviour of the core and edge plasma during this termination phase. The need for the modification of the main plasma transport model when the plasma evolves from H-mode to L-mode is due to the under-prediction of the edge plasma transport level by GLF23 (and correspondingly by the BgB-H-mode model tuned to it) and other gyrofluid and gyrokinetic turbulence-based transport models, which is usually referred to as the "edge transport shortfall" [29]. On the contrary, discharges with a long Type III H-mode phase can be modelled while keeping the core transport H-mode like (BgB-H-mode) until the H-L transition, as shown in Fig.11. In this case the level of transport at the plasma edge during the Type III ELMy H-mode phase is set an intermediate level between that required to model the Type I ELMy H-mode transport barrier and that expected in this region for L-mode transport. Finally, when the H-L transition takes place, a change of the core transport model to BgB-L-mode is required to model the remaining plasma evolution in a similar fashion to the discharges with the short Type III ELMy H-mode phase described above.

The independent verification of the modelling assumptions that are applied to model JET-C plasmas [3] and that will be used for ITER modelling in the next section, demonstrates that these assumptions are robust in the prediction of plasma behaviour in the Type I ELMy H-mode termination phase, at least as far as it concerns JET-C experiments, and can be therefore be applied with some confidence for the prediction of plasma behaviour in ITER during the termination phase of $Q_{DT}=$ 10 plasmas.

4. MODELLING OF SUDDEN H-L TRANSITIONS IN ITER Q_{DT} =10 SCENARIOS AND COMPARISON WITH EXPECTATIONS FROM JET-C PLASMA BEHAVIOUR

Modelling of ITER plasma behaviour during sudden decreases of the additional heating power level

has been carried out for 15MA $Q_{DT} = 10$ plasmas with the JINTRAC modelling code suite with similar physics modelling assumptions to those described in Section 3. The assumptions are summarized here, for convenience: a) Type I ELMy H-mode core plasma energy and particle transport is modelled with the GLF23 (or BgB-H-mode) transport model together with a reduction of energy and particle transport to neoclassical-like level in the transport barrier [28], b) During the transient H-mode phase following the step down of the additional heating level, and while the edge power flow level is above the L-H transition power, core transport is modelled with the GLF23 (or BgB-H-mode) transport models, c) During the H-mode transient phase, transport in the edge transport barrier is increased to an intermediate level between that required to model the Type I ELMy H-mode phase and that of the L-mode. The level itself depends on the margin of the time-averaged edge power flow above the L-H threshold power [3], d) Finally, when the edge time-averaged power flow drops under the L-H transition power the edge transport barrier is eliminated and the plasma transport model is assumed to change from GLF23 (or BgB-H-mode) to BgB-L-mode. With this assumption the H-L transitions obtained in the ITER simulations below usually have a dithering phase in which the plasma jumps between L-mode and H-mode confinement, phase in which it already has a rather deteriorated confinement, for up to typically 1s. For simplicity, in the rest of this section we take the middle time point of this ~ 1s dithering phase as the reference time for the H-L transition. In our simulations we further assume that neutral penetration through the divertor and SOL plasma in ITER (not modelled in this study) is very inefficient so that neutral fuelling of the core plasma by recycled particles is negligible and plasma fuelling is entirely provided by pellet injection. This is consistent with the findings of edge plasma simulations for ITER showing a very small neutral source in the confined plasma by recycling neutrals [13, 14] and the expected much higher fuelling efficiency by pellets than by gas fuelling and recycling in ITER [23]. In addition to the transport assumption above, in the modelling studies in this section we further assume that ELM control is maintained throughout the collapse phase of the Type I H-mode so that long ELM-free periods are avoided during this phase (this is simulated by applying a continuous ELM model [28]). An initial assessment of the consequences of failure to maintain ELM control in the sudden terminations of Type I ELMy H-modes for $Q_{DT} = 10$ plasmas in ITER is presented in Sect.5. It should be noted that in the modelling for ITER presented in this section the specific aspects related to increased W peaking and/or strong core W radiation during the H-mode collapse phase with controlled Type I ELMs and Type III ELMs are not included. A detailed modelling study to investigate W behaviour during the H-mode collapse phase in ITER will be carried out in the near future following a similar approach to that in [1]. An increased level of W radiation in the ITER H-mode collapse could shorten the timescale for the collapse of the plasma energy due to the reduced edge power flow and shorter Type III phases expected in such conditions.

In first place the ITER plasma behaviour has been modelled for the reference case in which both the additional heating and pellet fuelling are suddenly switched off during the stationary phase of an ITER 15MA $Q_{DT} \sim 10$ plasma with $P_{add} = 40MW$. As shown in Fig.12, after the switch off of

the additional heating and pellet fuelling, both plasma temperature and density start to decrease, as expected from the lack of additional heating and the negligible efficiency of the recycling flux to fuel the plasma assumed. The decrease of the temperature and density leads to a decrease of the alpha heating power while that of the density alone reduces the H-mode threshold power. As a result of this, the edge power flow, which is determined by the alpha heating and the derivative of the plasma energy, remains above the H mode threshold for approximately 7.0s, which is about twice $\tau_{E,H\text{-mode}}^{\text{flat-top}}$. During this high performance H-mode termination phase the plasma confinement evolves from values typical of Type I ELMy H-mode to L-mode-like values and we will call it, by analogy to the JET-C results, the "Type III ELMy H-mode phase" although in the ITER modelling no model for the Type III ELMs events is included. Consistent with a long duration of the Type III ELMy H-mode phase, the rate of decrease of the plasma energy remains relatively long with $\tau_W \sim 5.2$s, i.e. $\tau_W/\tau_{E,H\text{-mode}}^{\text{flat-top}} \sim 1.5$. The facts that: a) alpha heating is dominant in these ITER plasmas, b) alpha heating is not suddenly terminated when the additional heating is switched off and c) the slowing down time of fast particles (from NBI and alpha particles) has a timescale of few seconds play a key role in maintaining the plasma in the Type III ELMy H-mode phase in these ITER simulations. This is illustrated in Fig.13 where alpha heating is (artificially) terminated together with the additional heating in the simulation. In this case the duration of the Type III ELMy H-mode phase is reduced to 2.7s, about a factor of 3 shorter than when alpha heating is maintained (see Fig.12) and, correspondingly, the rate of decrease of the plasma energy is much faster with $\tau_W \sim 2.3$ s (i.e. $\tau_W/\tau_{E,H\text{-mode}}^{\text{flat-top}} \sim 2/3$).

Operational strategies after the sudden step down of the additional heating in ITER 15MA Q_{DT} = 10 plasmas can have a profound influence on the timescale of the decrease of the plasma energy in a way that is qualitatively similar to that observed in JET-C experiments [3]. In the case of ITER high Q_{DT} plasmas the concomitant effects of the operational strategies both on the evolution of the alpha heating and on the H-mode power threshold can lead to large quantitative differences both in the duration of Type III ELMy H-mode phase and in the timescale for the plasma energy reduction t_W. This is illustrated in Fig.14 where the reference simulation of Fig.11 is compared with two other simulations: one in which the plasma density is maintained by pellet fuelling after the switch off of the additional heating an another one in which the additional heating is not fully switched off but step down from 40 to 16.5MW. As shown in Fig.14, maintaining the plasma density after the additional heating switch off has a relatively small effect on the initial alpha heating power evolution but has a large effect on the H-mode threshold power because of the higher plasma density. This leads to a shorter duration of the Type III ELMy H-mode phase (3.8s to be compared with 7.0s in the reference case) and a shorter τ_W (4s instead of 5.2s in the reference case). During the Type III ELMy H-mode phase the plasma temperature remains above 10keV and, correspondingly, the alpha heating power (which comes predominantly from the core region) is similar for the simulations in which fuelling is maintained and those in which fuelling is stopped. On the other hand, maintaining a low level of additional heating in the collapse of Q_{DT} = 10 H-modes (16.5MW in Fig.14), together with the

stop of pellet fuelling can lengthen significantly the duration of the Type III ELMy H-mode phase (15s to be compared with 7s in the reference case). This is direct result of the increase of the edge power flow level by the remaining low level of additional heating   but also indirectly through its effect on the alpha heating as H-mode energy confinement is maintained. As a result, the timescale for the decrease of the plasma energy increases substantially and reaches $\tau_W \sim 10s$ when 16.5MW of NBI are maintained, to be compared with 5.2s in the reference case where all additional heating is stopped.

These modelling results indicate that operational strategies already applied to control the termination of high confinement H-mode plasmas in present experiments when the additional heating systems malfunction, such as stopping the fuelling and maintaining a low level of additional heating whenever possible, should be emulated in ITER in order to control the termination of Q_{DT} = 10 plasmas in similar circumstances. The additional heating level that will be available for DT operation in ITER is 73MW with three heating schemes (33MW NBI, 20MW ICRH and 20MW of ECRH) while ~ 40–50MW is foreseen for Q_{DT} = 10 operation. Therefore, even in the event of malfunction of one or two heating schemes, it may be possible to maintain additional heating to the plasma at a level of 10–20MW during the H-mode collapse phase of Q_{DT} = 10 plasmas (in the simulations of Fig.14 one NBI box with injected power of 16.5MW has been kept after the step down). This has the potential to mitigate considerably the issues related to the plasma position control and power fluxes to PFCs during this phase, as it allows the plasma to remain in the Type III ELMy H-mode for very long periods ($\sim 4.5\tau_E$) and for the plasma energy to decrease with very long timescales ($\sim 3\tau_E$) for which plasma radial position control can be easily maintained.

The quantitative accuracy of the overall plasma evolution predicted in these ITER simulations and the robustness of the conclusions extracted from it depend on the appropriate description of key details of the predicted plasma behaviour which, in turn, define the confinement properties of the plasma and its subsequent evolution. This detailed behaviour is a direct consequence of the physics assumptions utilized in the modelling of the H-mode plasma collapse phase. It is thus important to assess if the detailed plasma behaviour predicted for ITER is in good agreement with that observed experimentally at JET-C in similar conditions, while taking into account the specific features of these plasmas in ITER, i.e. the role of alpha heating. As an example, we compare in Fig.15 the time evolution of the total plasma energy and edge and core electron pressures (normalized to their flat top value) versus time (normalized to $\tau_{E,H\text{-mode}}^{\text{flat-top}}$) for a JET-C discharge with a long Type III ELMy H-mode phase and two ITER simulations with shorter and longer Type III ELMy H-mode phases respectively. As shown in Fig.15, the evolution of the JET-C plasma parameters in the collapse of the Type I ELMy H-mode is comprised between the two ITER simulations, as expected from the longer and shorter Type III ELMy H-mode phases in the ITER simulations. Although the overall plasma pressure and plasma energy evolution of the JET-C discharge are well bound by the ITER simulations, it is clear that some of the details of the pedestal evolution between this JET-C discharge and the ITER simulations differ qualitatively. For instance, while the degradation of the plasma

pedestal pressure is gradual in the Type III ELMy phase in the JET-C discharge and in the ITER simulations with a long Type III phase, the initial change in the pedestal pressure from the Type I to the Type III ELMy H-mode is more sudden in the JET-C pulse than in the ITER simulations. This is due to the fact that we assume that ELM control is maintained throughout the H-mode collapse phase in the ITER simulations while in the JET-C discharge no ELM control scheme was applied. As a result of this, the normalized (to the total plasma energy) energy loss of the last Type I ELM in JET-C was $\Delta W_{ELM}/W_{plasma} \sim 5\%$ to be compared with the less than 0.3% which is required to avoid unacceptable erosion of the ITER W divertor [20].

More generally, a comparison of the magnitude of the changes of the plasma parameters during the H-mode termination phase and of their characteristic timescales in the JET-C discharges analysed in Section 2 and in the ITER simulations described in this section is shown in Fig 16(a–c). This comparison indicates that, although some of the details of the evolution of the JET-C plasmas during the H-mode termination phase and the ITER simulations are not identical, as shown above, the overall predicted evolution of the main plasma parameters in the ITER simulations is surprisingly similar to that expected from a direct empirical extrapolation from the JET-C experimental results. The key parameter required for this empirical extrapolation is the edge power flow margin above the H-mode power threshold at the end of the Type I ELMy H-mode which determines the duration of the Type III ELMy H-mode phase, which in turn determines the magnitude of the drop of energy, density, etc. in this phase and their timescales. It is particularly interesting to see that the predicted density behaviour is similar in the JET-C discharges and in the ITER simulations despite the large differences in the expected fuelling of the plasma by the recycling fluxes during this phase in JET-C and in ITER and the simple modelling assumptions adopted for ITER in our study. As shown above, the detailed behaviour of the plasma density in the H-mode termination phase is crucial for the overall evolution of the plasma in this phase as it can influence the alpha heating level and is also the key parameter determining the evolution of the H-mode threshold power in the transient phase. The features of the density evolution will therefore be described in more detail below.

The similarity between the experimental plasma behaviour at JET-C and that modelled for ITER provides confidence that the predicted plasma behaviour for ITER plasmas is well founded on experimental results and that the operational strategies considered in this section to mitigate the power fluxes to PFCs and radial position control problems in the sudden termination of high Q_{DT} H-modes will be successful in ITER as well. The results presented here are only a first step in this direction. Further modelling of specific aspects of these termination phases and validation with experiment are required, particularly those related to the control of power fluxes to PFCs beyond those due to radial position control, which we have considered in this study, and impurity accumulation. The former is expected to require accurate control of the separatrix density in these transitions to ensure that the radiative divertor conditions are maintained to provide both acceptable power loads and low W sputtering production, while the latter may require, in addition, control of the relative scale lengths of the core density and temperature profiles in this phase. These two scale lengths are

12

found to determine whether impurities will accumulate or not in the core of H-mode plasmas [1, 2]. This control will have to be provided by the application of the additional heating and fuelling schemes at ITER during the H-mode termination phase. In addition, it should be noted that ELM control should be provided throughout the H-mode termination phase to ensure that both the ELM transient power pulses remain within the limits required to avoid unacceptable divertor erosion and to provide appropriate impurity exhaust from the core plasma.

As mentioned above, it is of particular interest the fact that the density decrease in the Type III ELMy H-mode phase is similar in these JET-C experiments and in the ITER simulations for which fuelling and plasma heating are suddenly stopped, even if the effectiveness of the recycling flux in JET-C and in ITER to fuel the plasma during this phase are expected to be very different. A detailed assessment of this issue requires fully integrated core-edge plasma simulations for both JET-C and ITER to quantitatively evaluate the particle outflux from the confined plasma in the H-mode termination phase, its amplification by ionization in the SOL and divertor and removal by divertor pumping and the resulting fuelling of the core plasma by the recycling flux. The local ionization in the SOL/divertor and divertor pumping will determine the separatrix density level while the balance between outflux and core plasma fuelling will determine the further evolution of the core density profile in the H-mode termination phase. Such simulations are beyond the scope of our study but are presently being carried out and their results will be described in [29]. In the present study we provide an initial assessment of the physics processes that lead to such a similar density evolution in JET-C and ITER during the H-mode termination phase despite the large expected differences in recycling flux behaviour pointed out above. The final confirmation of our findings below will come when the studies in [30] are completed.

The ITER simulations in this study have been performed including only the core plasma, assume that the separatrix density remains constant during this phase and that the effectiveness of the recycled flux to fuel the core plasma is zero (i.e. no neutral influx into the core plasma during this phase). In practice this means that the divertor pumping capability in ITER should be sufficient to remove the increased plasma outflux during the termination of the high Q_{DT} H-mode thus preventing the transient accumulation of particles in the SOL during this phase, which would increase the separatrix density and slow down the core plasma density decay. While a quantitative assessment of this phenomenology awaits the results of the on-going integrated plasma core-edge simulations for ITER [30], it is important to note that for the expected duration of the Type III ELMy H-mode phase of ~ 7s and a decrease of the plasma density by a factor of ~ 2 during this phase, as shown in Fig.16, the plasma outflux rate in ITER during the H-mode termination phase is $\sim 7 \times 10^{21}$ s^{-1}. This outflux is an order of magnitude smaller than the pumped flux during the stationary plasma phase of the $Q_{DT} = 10$ plasmas in ITER, which is $\sim 10^{23}$ s^{-1}. Obviously what will be the achievable pumped flux during the H-mode termination phase in ITER requires detailed modelling as described above. However, on the basis of simple extrapolations based on the high recycling divertor scaling, which predict that the neutral pressure at the divertor and thus the pumped flux scales with n_{sep}^2 [16], a

pumped flux of $\sim 10^{22}$ s^{-1} during the transient H-mode termination phase should be achievable in ITER provided that the separatrix density during the transient phase is not lower than a factor of 3 that of the burning plasma phase. Analysis of the divertor neutral pressure measurements during the H-mode termination phase at JET-C indicates that indeed sufficient pumping is provided by the divertor at JET-C to prevent a large increase of the edge density due insufficient particle removal during this phase. This is shown in Fig.17 where the sub-divertor neutral pressure evolution and the associated divertor pumped flux are compared with the rate of decrease of the total core plasma particle content, as evaluated from the High Resolution Thomson scattering measurements. As seen in Fig.17, except for a short initial phase lasting ~50ms in which the rate of decrease of the core plasma particle content may exceed the pumped flux, for the rest of the Type III ELMy H-mode phase lasting 550ms the pumped divertor flux is similar (usually larger) than the rate of decrease of the core plasma particle content. It should be noted that, due to the conductance between the sub-divertor volume and the location of the penning gauge from which the neutral pressure is determined, there is a delay of ~150-200 ms between changes of the neutral pressure at the divertor cryo-pump and at the penning gauge [10]. In addition, for the same reason, fast transients in the neutral pressure at the divertor cryo-pump cannot be measured. To account for the effect of this delay, the pumped flux in Fig.17 has been evaluated both based on the penning gauge neutral pressure measurement (assuming balance between the fuel input and the fuel output in the stationary phase of the H-mode) and on the penning gage neutral pressure measurement shifted 200ms earlier in time.

5. INITIAL EVALUATION OF THE CONSEQUENCES OF FAILURE OF ELM CONTROL DURING FAST H-L TRANSITIONS IN THE ITER Q_{DT} = 10 SCENARIO

As mentioned above, in the ITER simulations in Section 4 we have considered that ELM control can be sustained during the Type I H-mode collapse phase down to the Type III ELMy H-mode. In ITER there may be occasions where ELM control is lost during this phase leading to a final large Type I ELM similar to those in the JET-C discharges in Figs.2 and 7. To study what would be the expected plasma evolution in these circumstances in ITER a set of simulations has been performed in which a large decrease of the plasma energy (simulating a large ELM) takes place at the switch off of the additional heating. To simulate this, the reduction of transport at the plasma edge associated with H-mode confinement is removed for a short period (~20ms), which leads to a sudden decrease of the plasma energy by $\sim$ 50MJ (i.e. ΔW_{ELM} = 50 MJ or $\Delta W_{ELM}/W_{plasma} \sim 14\%$ in ITER). As expected from the results discussed in the previous section, the lower W_{plasma} after this ELM event reduces the edge power flow (both directly because of the decrease of W_{plasma} and indirectly by the decrease in alpha heating) which leads to a shortening of the Type III ELMy H-mode to 5.4s (lower edge power flow margin above the H-mode threshold) with respect to the reference 7s when ELM control is maintained (see Fig.12), as shown in Fig.18. This leads to a faster time scale for the energy decay in the H-mode termination phase of $\tau_w \sim 4.2$s instead of the reference 5.2s.

The simulation above, however, does not reflect the real plasma behaviour that is to be expected

14

in ITER in such circumstances because it does not take into account the consequences of the large W impurity influx that will enter the core plasma following such large ELM. A large ELM with ΔW_{ELM} in the 10's of MJ in ITER will cause considerable power and particle fluxes to the PFCs that will lead to a significant W influx to be produced at the ITER divertor. In first place it should be noted to for such large ELMs significant melting of the W divertor is expected and, therefore, they should be avoided/controlled in ITER by application of the ELM control schemes included in the ITER baseline [20]. But even if W melting were to be avoided (for instance if the ELM wetted area would increase to several 10's of square meters in ITER for such large ELMs), the production of W by physical sputtering alone during such ELMs is significant. Modelling of the SOL and edge plasma behaviour (up to $\rho \sim 0.8$) during stationary phases of the ITER $Q_{DT} = 10$ scenario with the SOLPS code suite has shown that the divertor physical sputtering W source from large ELMs (of several MJs) leads to an influx of W into the confined plasma after such ELMs that increases core radiation and leads to a decrease of the separatrix temperature to ~10eV, which is followed by a radiative collapse of the ITER plasma solution [5]. In order to determine if such radiative collapse of the plasma by W radiation would also take place during the termination phase of ITER $Q_{DT} = 10$ H-mode plasmas when ELM control is lost, we have carried out core plasma simulations in which we prescribe a W influx into the core plasma in a range of 2–6 10^{19} W atoms during a period of 0.1-0.3s following a large Type I ELM with $DW_{ELM} = 40$ MJ. The magnitude of this core W influx is in agreement with predictions from edge plasma simulations for ITER [5] scaled up to $\Delta W_{ELM} = 40$MJ. For the largest W influxes the core plasma radiation increases very suddenly following the ELM leading to a fast decrease of the plasma energy and of the edge power flow, which in turn causes a fast return of the plasma to L-mode confinement and very shortly after that there is a radiative collapse of the solution. This behaviour is analogous to that found in [Coster 2013] and would correspond to a disruption in the experiment.

For the lower range of W influxes it is possible to prevent the final radiation collapse and to obtain a simulation in which the energy of the plasma decreases in very fast timescales $\tau_w \sim 0.8$s (even faster than the worst case scenario proposed initially for ITER for fast H-L transitions [16]), as shown in Fig.19. To obtain these results it is necessary to assume that, in the Type III ELMy H-mode phase and after the transition to L-mode, the diffusion coefficient of W is very large ($D_W = (3-5) \times D_{DT}^{BgB-L-mode}$, where $D_{DT}^{BgB-L-mode}$ is the diffusion coefficient from the Bohm-gyroBohm model for DT ions) so that W is quickly removed from the plasma edge and the radiative collapse of the simulation is avoided. It is not clear if this is a physically justifiable assumption, as it is usually found that impurities are subject to a similar level of anomalous transport to that of the main ions [1, 2]. Although the radial movement of the plasma will be significant in ITER for the conditions simulated in Fig.19 given the extremely short timescale in which the plasma energy collapses, the power flow that can potentially be intersected by the first wall components at the high field side is expected to be very modest (under 10–20MW for most of the collapse in the simulation in Fig.19). There is only a short lived period of less than 1s duration during the H-mode collapse phase in

which there is a significant power outflow (~ 80MW), which is expected to be deposited at the divertor target. These values compare very favourably with the originally foreseen edge power flow of 150–200MW decreasing exponentially with a time scale of 1.8 s where significant power fluxes to the first wall were expected [18].

On the basis of these simulations we cannot exclude that lack of ELM control in the termination phase of high Q_{DT} H-modes in ITER and the ensuing W influxes might lead to a fast decrease of the plasma energy and a significant radial inwards movement of the plasma while avoiding the disruption in some specific circumstances. For the vast majority of cases, however, a radiative collapse of the plasma and an ensuing disruption following the W influx, which will be mitigated by the ITER disruption mitigation system, will occur. Even in the cases in which non-disruptive plasma contact between the plasma and the inner wall might occur, the expected power fluxes to PFCs at this location are not expected to have major consequences. The W influx caused by the uncontrolled ELM during the termination of the ITER $Q_{DT} = 10$ H-mode plasma will lead to most of the plasma energy to be radiated so that the resulting power fluxes to the inner wall PFCs are expected to be rather moderate. A quantitative evaluation of these power fluxes requires self-consistent simulations of the plasma behaviour during the H-mode termination phase together with an appropriate free-boundary model of the plasma equilibrium and magnetic control schemes and actuators in ITER, which are presently being carried out. In addition, as already mentioned above, due to the large possible erosion and melting of the W divertor target in these uncontrolled events it is likely that fast plasma termination schemes, akin to disruption mitigation, will be applied when such failures of ELM control in the termination phase of high Q_{DT} H-modes are detected in ITER.

6. SUMMARY, DISCUSSIONS AND CONCLUSIONS

JET-C discharges in which the high performance H-mode phase is suddenly terminated by the switch off of additional heating and plasma fuelling have been analyzed with a view to provide a physics basis to evaluate plasma behaviour in ITER in similar circumstances. The analysis of these experiments reveals that the timescale for the decrease of the plasma energy in this termination phase is correlated with the duration of the Type III ELMy H-mode phase between the last Type I ELM and the H-L transition. The longer the Type III ELMy H-mode phase duration, the longer the timescale for plasma energy collapse. The duration of the Type III ELMy H-mode phase is mainly determined by the ratio of the edge power flow to the H-mode threshold power at the beginning of this phase, with the larger ratios leading to the longer Type III ELMy H-mode durations.

Modelling for ITER, with modelling assumptions that have been derived from the JET-C experiments, shows that for $Q_{DT} = 10$ discharges the expected timescale for energy decay after a sudden additional heating and fuelling switch off is expected to be longer than the energy confinement time during the burning phase, provided that ELM control can be maintained during this phase. This is in contrast to simple expectations based on an instantaneous return to L-mode, which provides a timescale a factor of ~2 faster than the energy confinement time during the burning phase. The

reason for this much longer timescale for the decay of plasma energy in the H-mode termination phase is the fact that the simulated ITER plasma remains in an equivalent condition to that of the Type III ELMy H-mode in experiments due to the combined effect of the alpha heating (which decays slowly) and the decrease of the density (and thus of the H-mode threshold power), which keeps the plasma in H-mode for very long periods. Removing (artificially) the alpha heating together with the additional heating and plasma fuelling leads to a shortening of the equivalent of the Type III ELMy H-mode phase in ITER and to a much faster collapse of the plasma energy which approaches (only 40% larger) the timescales expected from an immediate return to L-mode. Operational strategies to control the duration of the Type III ELMy H-mode phase in ITER, and thus of the timescale of energy decay, based on plasma fuelling control and a maintaining a low level of additional heating after the main power step-down have been found to be effective and are, in principle, feasible in practice, although the implications for W accumulation and their consequences on the Type III ELMy H-mode duration remain to be evaluated

An initial evaluation of the consequences of the lack of ELM control during these fast $Q_{DT} = 10$ H-mode terminations in ITER has been carried out. The effect of the lack of ELM control on the rate of decrease of the plasma energy has been found to be moderate (even for ELM energy losses of 50MJ), provided that the uncontrolled ELMs do not cause a significant influx of W into the main plasma. However, even under the rather optimistic assumption that the only mechanism for W production during such large ELMs is physical sputtering (in reality significant W evaporation and melting are expected to occur during such ELMs) the associated W influxes into the main plasma are found to lead to the radiative collapse of the plasma in timescales shorter than 0.5s, which in the experiment would correspond to a disruption. For influxes in the lower range of expectations and specific W transport assumptions, the radiative collapse is avoided and the W radiation only causes a sudden termination of the H-mode phase and a very fast decrease of the plasma energy with timescales of ~0.8s. Such event will cause a large radial displacement of the plasma in ITER, which is difficult to control on these timescales, but is not expected to lead to large power fluxes to the first wall PFCs at the high field side as most of the plasma energy is lost by radiation rather than by conduction to the first wall PFCs.

Further progress in the evaluation of H-mode terminations in ITER requires both improvements on the physics basis by validation with new experiments and of the models. A selection of these required improvements (some already under development) are described below:

a) A more advanced physics-based criterion is required for the determination of the conditions at which the plasma returns from H-mode to L-mode. This is implemented in the ITER modelling presented in this paper on the basis of the H-mode threshold power, which is in agreement with the experimental determination of the H-L power threshold in JET [21]. For such a dynamic situation as considered here this prescription provides a good overall description of the experimental results but significant scatter remains, which indicates that

there are additional factors to the margin above the H-mode power threshold that determine whether the plasma remains in H-mode or not. A more experimentally substantiated physics-based criterion for the H-L transition, probably on the basis of edge plasma parameters such as density, temperature, pressure or pressure gradient, electric field, etc., would be required to reduce the uncertainty in the ITER modelling in this area.

b) An improved model for the expected level of pedestal transport in the transient Type III ELMy H-mode during the termination phase. In the modelling presented in this paper this is evaluated to be at an intermediate value between that of the Type I ELMy H-mode and that of the L-mode and it is thus linked to the to the margin above the H-mode power threshold in the modelling, which is found to reproduce reasonably well the experiments. However, depending on the precise value of this intermediate value, the core plasma collapse will take place on a shorter or longer timescale. Therefore an adequate characterization of plasma confinement in stationary and transient Type III ELMy H-modes and of its relation with operational conditions (margin above the H-mode power threshold, value of edge plasma density, temperature, edge electric field, etc.) is required to ensure that the predictions for ITER are accurate.

c) An improved understanding of particle transport (DT fuel and W impurity) and its dynamics during the H-mode collapse phase and of its integrated modelling. This concerns both core transport (the main issue being W impurity accumulation), as very peaked density profiles can develop in this phase, as well as edge transport and particle removal that can potentially influence the timescale for the decrease of the plasma density in ITER, which in turn affects both the H-mode threshold power and the alpha heating. In addition, for operational strategies in which long Type III phases are sustained to slow down the decrease of plasma energy, core impurity dynamics must be understood. A priori, the associated plasma conditions (peaked density profiles with decreasing plasma temperatures) are prone to W impurity accumulation, as found in JET-ILW experiments which are well reproduced by impurity transport models which include both neoclassical and anomalous transport [2], and the timescale of such possible accumulation compared to the Type III ELMy H-mode duration needs to be evaluated for ITER. This is important for ITER because, in addition to the W source from the divertor, impurity seeding will be used to control the divertor conditions in order to control both the divertor power loads and the W sputtering source and this control will need to be maintained during the transient phases as well.

d) Finally, for the prediction of the power fluxes to PFCs during the H-mode termination phase both integrated modelling of the ITER core and edge plasma are required as well as of the control of the plasma position during this phase. The latter is essential to predict the power fluxes that will reach the first wall components located on the high field side of the tokamak as the plasma moves radially inwards during the H-mode termination phase.

18

REFERENCES

[1]. Angioni, C., et al., Proc. 40th European Physical Society Conference on Plasma Physics, Espoo, Finland, 2013, paper P4.142, http://ocs.ciemat.es/EPS2013PAP/pdf/P4.142.pdf

[2]. Angioni, C., et al., accepted for publication in Nuclear Fusion 2014.

[3]. Belo, P. et al., Proc. 38th European Physical Society Conference on Plasma Physics, Strasbourg, France, 2011, paper P1.119, http://ocs.ciemat.es/EPS2011PAP/pdf/P1.119.pdf

[4]. Beurskens, M.N.A., et al., Nuclear Fusion **49** (2009) 125006.

[5]. Calabro, G., et al., Proc. 40th European Physical Society Conference on Plasma Physics, Espoo, Finland, 2013, paper O2.106, http://ocs.ciemat.es/EPS2013PAP/pdf/O2.106.pdf.

[6]. Coster, D.P., et al., Proc. 40th EPS Conference, Espoo, Finland, 2013, paper P1.104.

[7]. de Vries, P.C., et al., Plasma Physics and Controlled Fusion **54** (2012) 124032.

[8]. Erba, M., et al., Plasma Physics and Controlled Fusion **39** (1997) 261.

[9]. Gribov, Y., et al., Nuclear Fusion **47** (2007) S385.

[10]. Groebner R. J., et al., Nuclear Fusion **41** (2001) 1789.

[11]. Hillis, D.L., et al., Review of Scientific Instruments **70** (1999) 359.

[12]. ITER Physics Basis, Nuclear Fusion **39** (1999) 2137.

[13]. Kukushkin, A.S., et al., Nuclear Fusion **43** (2013) 716.

[14]. Kukushkin, A.S., et al., Nuclear Fusion **53** (2013) 123025.

[15]. Lister, J., et al., Proc. 40th European Physical Society Conference on Plasma Physics, Espoo, Finland, 2013, paper P1.164, http://ocs.ciemat.es/EPS2013PAP/pdf/P1.164.pdf

[16]. Loarte, A., et al., Nuclear Fusion **38** (1998) 331.

[17]. Loarte, A., et al., Plasma Physics and Controlled Fusion **44** (2002) 1815.

[18]. Loarte, A., et al., Proc. 22nd Int. Conf. on Fusion Energy 2008 (Geneva, Switzerland,2008) (Vienna: IAEA) IT/P6-13.

[19]. Loarte, A., et al., Nuclear Fusion **53** (2013) 1083031.

[20]. Loarte, A., et al., Nuclear Fusion **54** (2014) 033007.

[21]. Maggi, C.F. et al., Proc. 40th European Physical Society Conference on Plasma Physics, Espoo, Finland, 2013, paper P2.168, http://ocs.ciemat.es/EPS2013PAP/pdf/P2.168.pdf

[22]. Martin, Y.R., et al., Journal of Physics: Conference Series **123** (2008) 012033.

[23]. Maruyama, S., et al., 24th Fusion Energy Conference, San Diego, USA, 2012, paper ITR/P5-24 and http://www-naweb.iaea.org/napc/physics/FEC/FEC2012/index.htm.

[24]. Mitteau, R., et al., Physica Scripta **T145** (2011) 014081.

[25]. Nunes, I., et al., Nuclear Fusion **53** (2013) 073020.

[26]. Parail, V.V., Plasma Physics and Controlled Fusion **44** (2002) A63.

[27]. Parail, V.V., et al., 24th Fusion Energy Conference, San Diego, USA, 2012, paper ITR/P1-10 and http://www-naweb.iaea.org/napc/physics/FEC/FEC2012/index.htm.

[28]. Parail, V.V., et al., Nuclear Fusion **53** (2013) 113002.

[29]. Rhodes, T. L., et al., Nuclear Fusion **51** (2011) 063022.

[30]. Romanelli, M., et al. 25th Fusion Energy Conference, Saint Petersburg, Russian Federation, 2014.
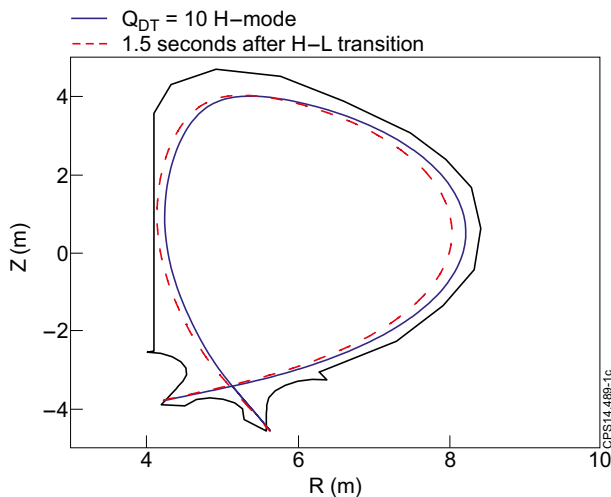
Figure 1: Radial plasma movement following a fast H-L transition in which plasma energy decreases with a ~ 2 s exponential decay time for an ITER $Q_{DT} = 10$ plasma [14].
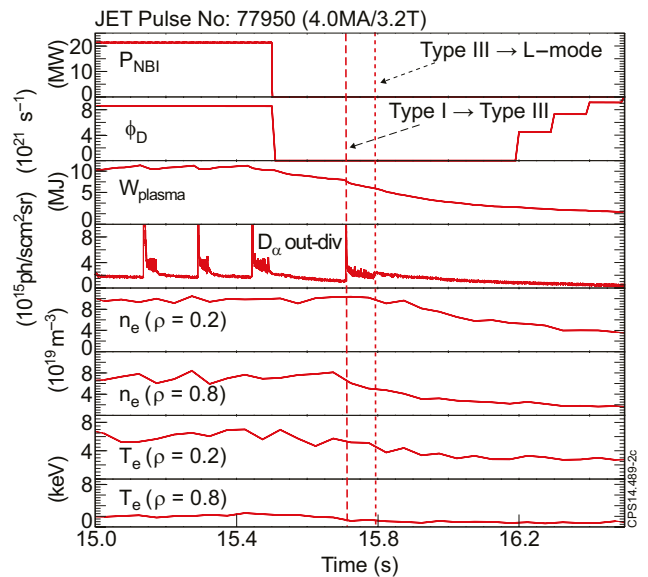
Figure 2: Evolution of the NBI heating power, gas fuelling rate, plasma energy divertor D_α flux and electron density and temperature at two radial locations ($\rho = r/a = 0.2$ and 0.8) for one of the JET-C discharges analyzed. The dashed lines show the times at which the plasma undergoes a transition from Type I to Type III ELMy H-mode and from Type III ELMy H-mode to L-mode respectively.
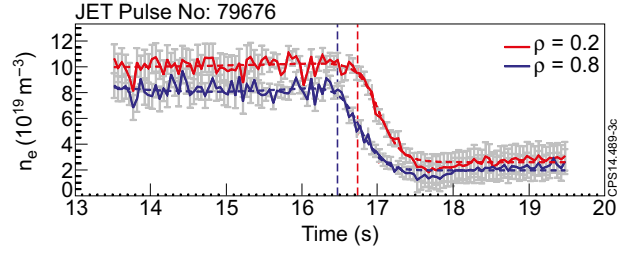
Figure 3: Evolution of the core (ρ = 0.2) (in red) and edge (ρ = 0.8) density (in blue) during the Type I ELMy H-mode termination phase for a 4.3MA JET-C plasma. The dashed lines show the times at which the plasma density starts to decrease at the core and the edge, as the plasma confinement transients from the Type I to the Type III ELMy H-mode regime.
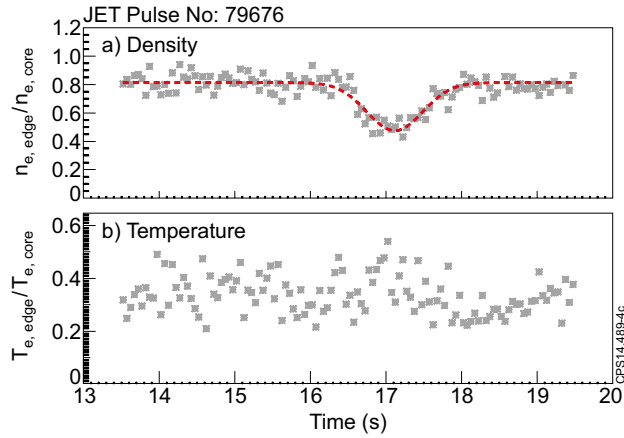
Figure 4: a) Evolution of the ratio of the edge (ρ = 0.8) to core (ρ = 0.2) density during the Type I ELMy H-mode termination phase for a 4.3 MA JET-C plasma showing the increased peaking of the density profiles during this phase. The dashed line shows a Gaussian fit utilized to characterized quantitatively the duration of this peaked density phase. b) Evolution of the ratio of the edge (ρ = 0.8) to core (ρ = 0.2) temperature during the Type I ELMy H-mode termination phase for a 4.3MA JET-C plasma showing no change in the peaking of the temperature profiles during this phase.
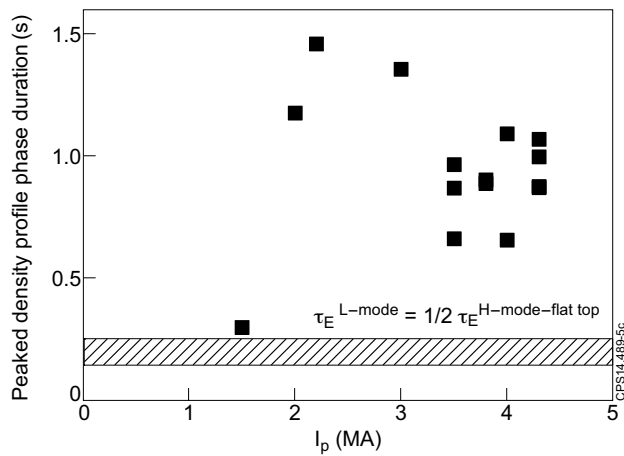
Figure 5: Duration of the peaked density profiles during the Type I ELMy H-mode termination phase versus plasma current at JET-C. The dashed band illustrates the typical range of the expected L-mode energy confinement time estimated as ½ of that during the flat top of these discharges of the discharges analyzed for reference.
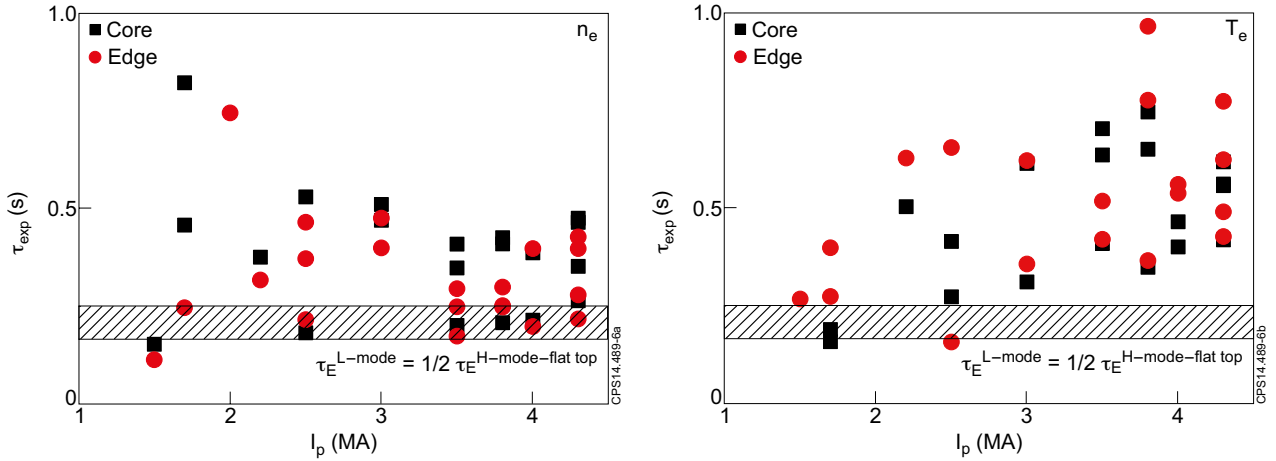
Figure 6: a) Timescale for the decrease of the edge ($\rho = 0.8$, red circles) and core ($\rho = 0.2$, black squares) density during the Type I ELMy H-mode termination phase versus I_p for the JET-C discharges considered. b) Timescale for the decrease of the edge ($\rho = 0.8$, red circles) and core ($\rho = 0.2$, black squares) temperature during the Type I ELMy H-mode termination phase versus I_p for the JET-C discharges considered. The dashed band illustrates the typical range of the expected L-mode energy confinement time estimated as ½ of that during the flat top of these discharges of the discharges analyzed for reference.
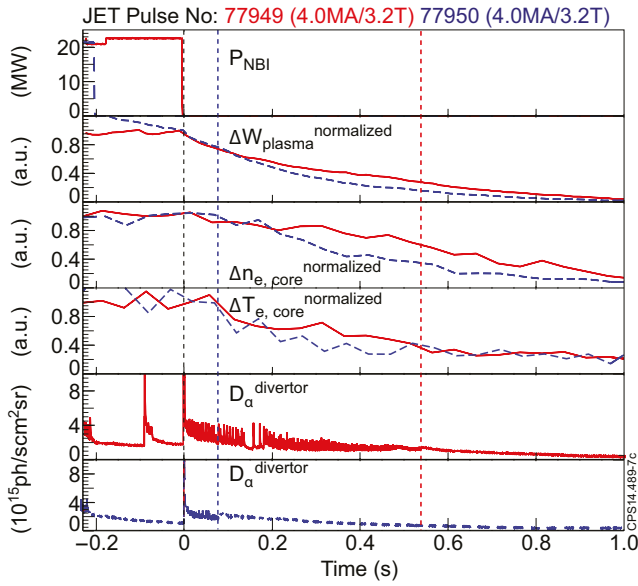
Figure 7: Evolution of the NBI heating power, normalized change of plasma energy, core ($\rho = 0.2$) electron density and temperature and divertor D_α flux for two similar JET discharges at high plasma current with very different duration of the Type III ELMy H-mode phase. The dashed coloured lines show the times at which the plasma undergoes a transition Type III ELMy H-mode to L-mode for both discharges. The changes in plasma energy, density and temperature are normalized to the respective changes between their values before the last Type I ELM and after the L-H transition, i.e. $(f(t)-f(t_{L-mode}))/(f(t_{Type-I})-f(t_{L-mode}))$ where f is the plasma energy, density or temperature respectively.

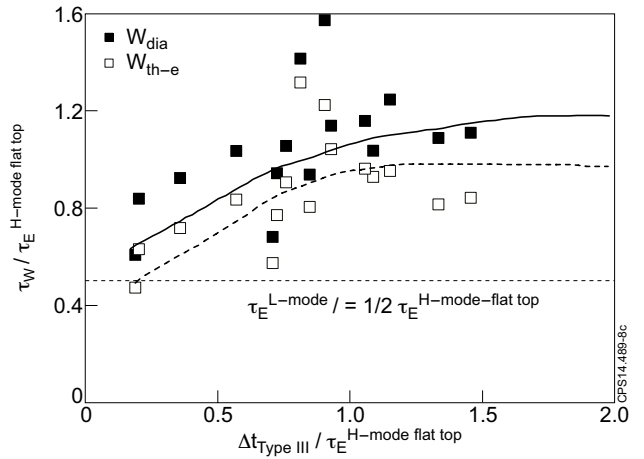*Figure 8: Normalized (to $\tau_E^{H\text{-}mode\;flat\text{-}top}$) timescale for the decrease of the plasma energy (as evaluated by the diamagnetic loop measurements) and of the electron energy (as evaluated by measurements of the High resolution Thomson Scattering) versus normalized duration of the Type III ELMy H-mode phase. The horizontal dashed line indicates the timescale expected on the basis of an immediate transition from Type I ELMy H-mode to L-mode (evaluated as $\tau_E^{L\text{-}mode} \sim ½\; \tau_E^{H\text{-}mode\;flat\text{-}top}$). The other lines are to guide the eye.*
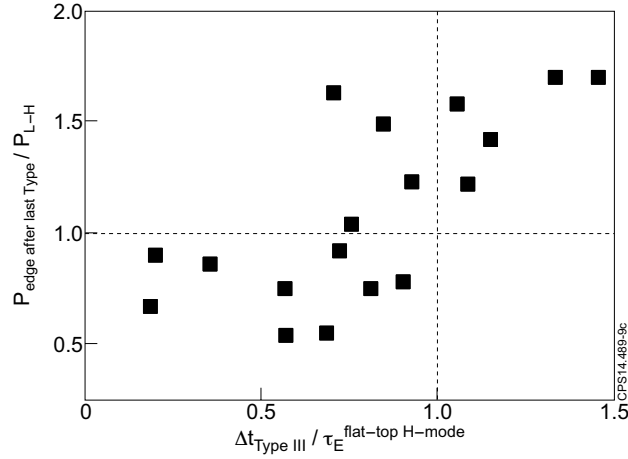
22

Figure 9: Normalized (to the H-mode power threshold) edge power flow after the last Type I ELM versus the normalized (to $\tau_E^{H\text{-}mode\,flat\text{-}top}$) duration of the Type III ELMy H-mode phase. The horizontal and vertical dashed lines indicate the points for which the edge power flow is equal to the H-mode threshold power and the points for which the duration of the Type III ELMy H-mode phase equals the energy confinement of the high performance H-mode phase in these discharges, respectively.
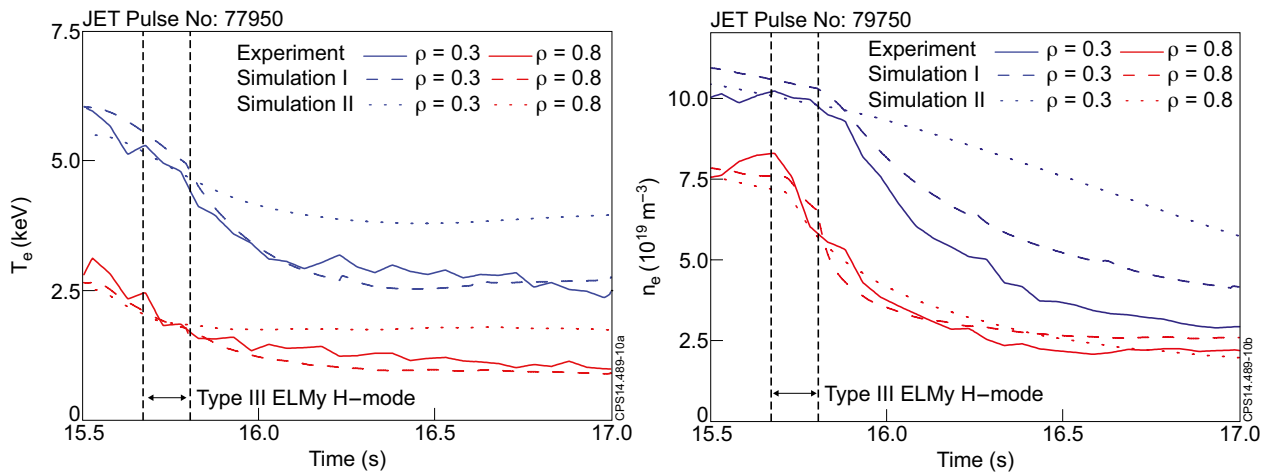

Figure 10: Measured and modelled edge and core temperature (a) and density (b) for a JET-C pulse with a short Type III ELMy H-mode phase. Two sets of ASTRA simulations have been performed: Simulation I in which the BgB-H-mode transport model is used for the H-mode phase and this is followed by a change to BgB-L-mode at the L-mode transition and Simulation II in which the BgB-H-mode transport model is also kept after the L-mode transition. Simulation I reproduces better the experimental measurements.
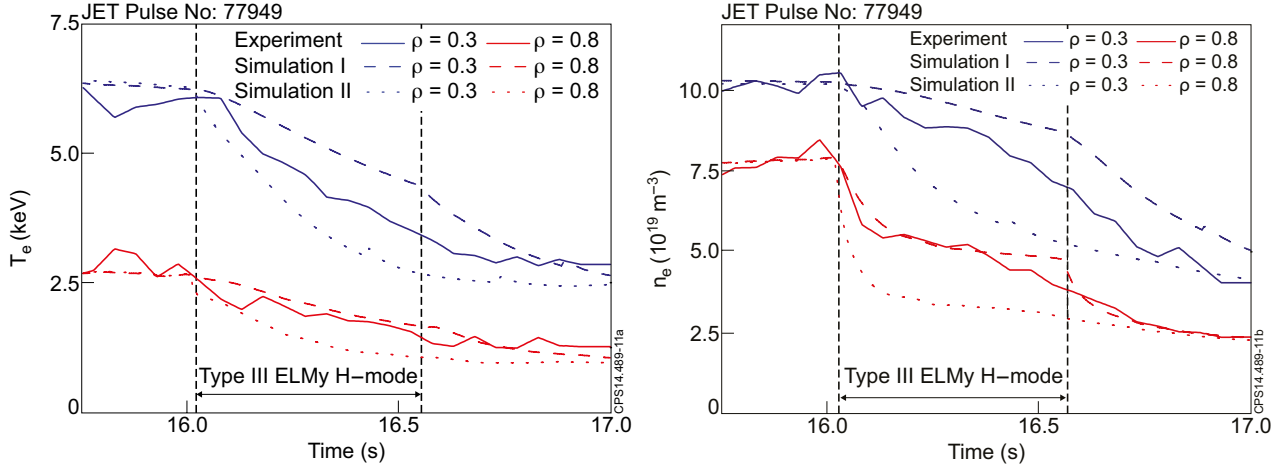
Figure 11: Measured and modelled edge and core temperature (a) and density (b) for a JET-C pulse with a long Type III ELMy H-mode phase. Two sets of ASTRA simulations have been performed: Simulation I in which the BgB-H-mode transport model is maintained until the end of the Type III ELMy H-mode phase (then followed by a change to BgB-L-mode) with edge transport at an intermediate level between the Type I ELMy H-mode and that of the L-mode and Simulation II in which the plasma transport is assumed to return to L-mode values at the beginning of the Type III H-mode phase. Simulation I reproduces better the experimental measurements.
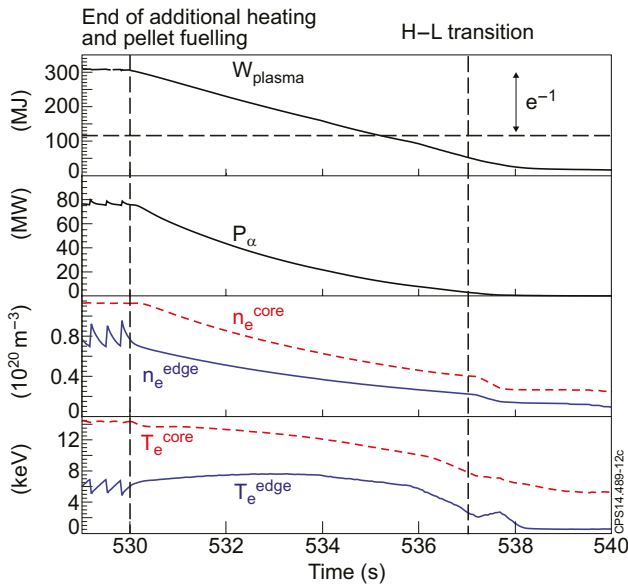
Figure 12: Modelling of the sudden termination of a Q_{DT} =10 H-mode plasma in ITER when additional heating and pellet fuelling are switched off at 530s (indicated by a dashed line). From top to bottom: plasma energy, alpha heating, core and pedestal density and temperature are displayed. The time at which the H-L transition takes place is indicated by a vertical dashed line; the time at which the plasma energy decreases by e^{-1} from its value during the stationary burning plasma phase (which defines τ_W) is indicated by the intersection of the horizontal dashed line with the time trace of the plasma energy.
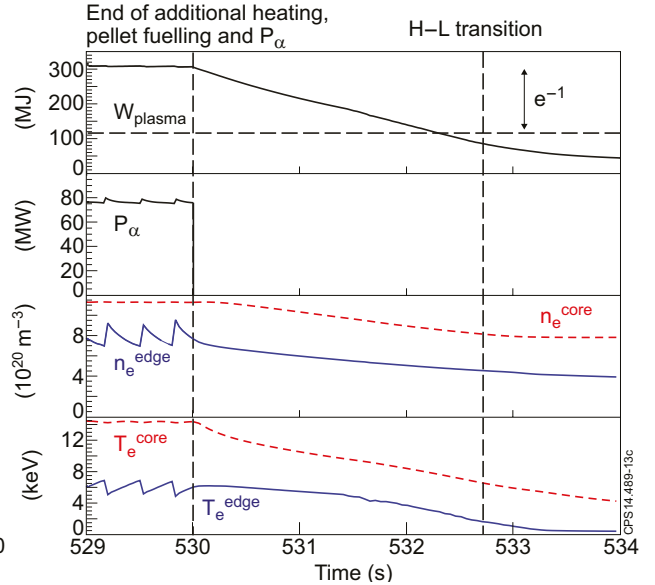
Figure 13: Modelling of the sudden termination of a Q_{DT} =10 H-mode plasma in ITER when additional heating, pellet fuelling and alpha heating are switched off at 530s (indicated by a dashed line). From top to bottom: plasma energy, alpha heating, core and pedestal density and temperature are displayed. The time at which the H-L transition takes place is indicated by a vertical dashed line; the time at which the plasma energy decreases by e^{-1} from its value during the stationary burning plasma phase (which defines τ_W) is indicated by the intersection of the horizontal dashed line with the time trace of the plasma energy. Note that the time span of the horizontal axis is a factor of ~2 smaller than in Fig.12 in accordance with the faster plasma evolution in this case.
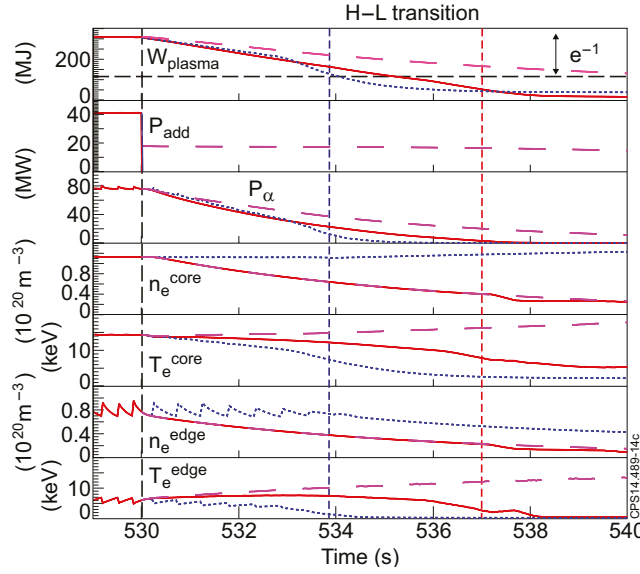
24

Figure 14: Modelling of the sudden termination of a $Q_{DT} = 10$ H-mode plasma in ITER. Three simulations are compared. In the first reference simulation in (red) additional heating and pellet fuelling are switched off at 530s (indicated by a dashed line). In the second simulation (blue) additional heating is switched off at 530s but the fuelling is maintained. In the third simulation (magenta) 16.5MW of NBI heating after 530s is maintained while pellet fuelling is stopped. From top to bottom: plasma energy, additional heating, alpha heating, core and pedestal density and core and pedestal temperature. The time at which the H-L transition takes place for the first and second simulation is indicated by a vertical dashed line; the time at which the plasma energy decreases by e^{-1} from its value during the stationary burning plasma phase (which defines τ_W) is indicated by the intersection of the horizontal dashed line with the time trace of the plasma energy for the three simulations.

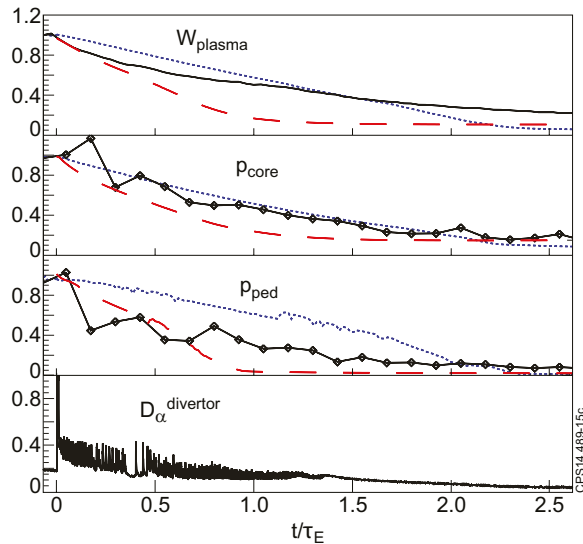*Figure 15: From top to bottom; evolution of the plasma energy (normalized to the flat top value), core and pedestal plasma pressure and divertor D_α (only for the JET-C discharge) in the H-mode collapse phase versus normalized time (to $\tau_{E,H\text{-}mode}^{flat\text{-}top}$) for Pulse No: 77949 (in black) and two ITER simulations: blue traces correspond to the simulation in Fig.12 and red traces to the simulation in Fig.13.*
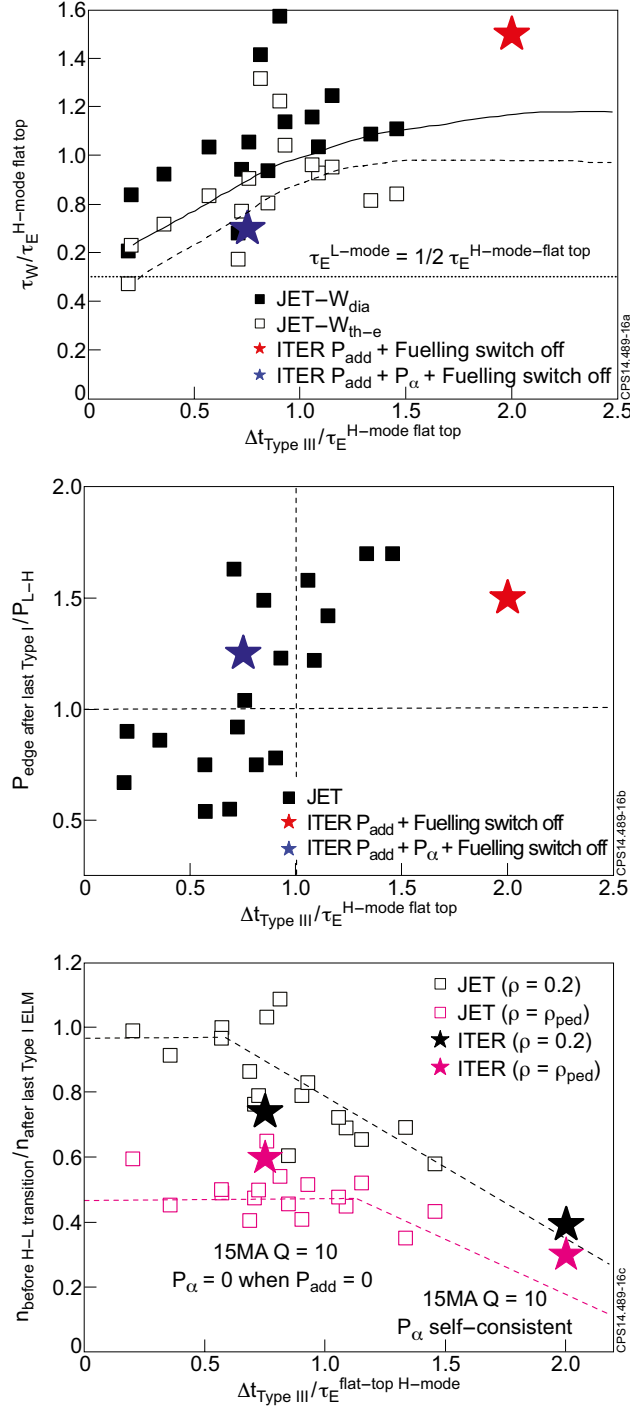
Figure 16: a) Normalized (to $\tau_E^{H\text{-}mode\,flat\text{-}top}$) timescale for the decrease of the plasma energy in the JET-C experiments and in the ITER simulations in Figs.12 and 13 versus the normalized (to $\tau_E^{H\text{-}mode\,flat\text{-}top}$) duration of the Type III ELMy H-mode phase. The horizontal dashed line indicates the timescale expected on the basis of an immediate transition from Type I ELMy H-mode to L-mode with $\tau_E^{L\text{-}mode} = 1/2\ \tau_E^{H\text{-}mode\,flat\text{-}top}$; the other lines are to guide the eye. b) Normalized (to the H-mode power threshold) edge power flow at the termination of the high confinement H-mode phase versus the normalized (to $\tau_E^{H\text{-}mode\,flat\text{-}top}$) duration of the Type III ELMy H-mode phase for the JET-C experiments and the ITER simulations in Figs.12 and 13 The horizontal and vertical dashed lines indicate the points for which the edge power flow is equal to the H-mode threshold power and the points for which the duration of the Type III ELMy H-mode phase equals the energy confinement of the high performance H-mode phase in these discharges, respectively. c) Normalized decrease of the plasma density at the plasma core ($\rho = 0.2$) and at the top of the pedestal ($\rho = \rho_{ped}$) versus the normalized (to $\tau_E^{H\text{-}mode\,flat\text{-}top}$) duration of the Type III ELMy H-mode phase for the JET-C experiments and the ITER simulations in Figs.12 and 13. The dashed lines are to guide the eye.
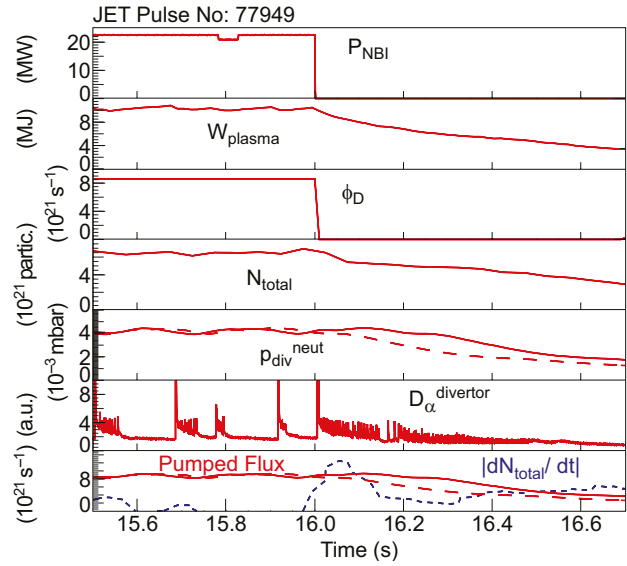
Figure 17: From top to bottom: NBI heating power, plasma energy, gas fuelling rate, total core plasma particle content, sub-divertor neutral pressure, divertor D_α, rate of decrease of the core plasma particle content particle and pumped flux by the divertor cryo-pump during a JET-C discharge with a long Type III ELMy H-mode phase. The pumped flux is evaluated by assuming that the gas + NBI fuelling is balanced by the pumped flux in the stationary phase of the discharge (i.e. before 16s). To evaluate the effect of the delay introduced by the connection between the gauge that measures the divertor pressure at JET-C and the neutral pressure at the pump that determines the instantaneous value of the pumped flux, the neutral pressure measurements have been shifted earlier in time by 200ms and the pumped flux evaluated accordingly. This is illustrated by the dashed lines in the neutral pressure and pumped flux plots. Good balance between the rate of decrease of the plasma particle content and the pumped flux is found during the Type III ELMy H-mode phase.
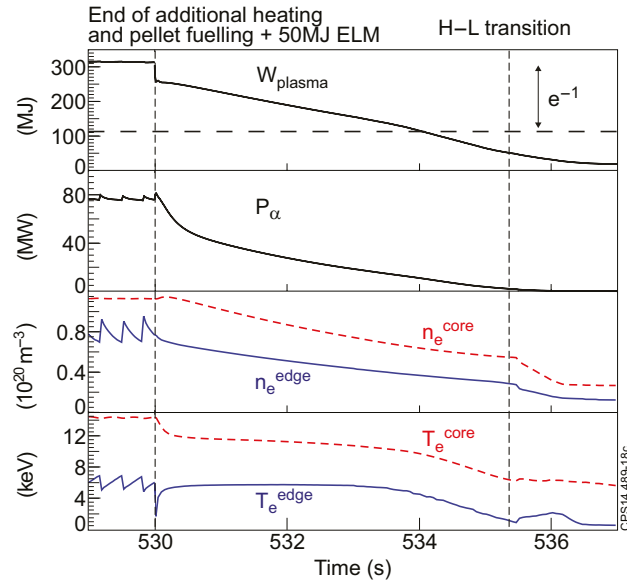

Figure 18: Modelling of the sudden termination of a $Q_{DT} = 10$ H-mode plasma in ITER when additional heating and pellet fuelling are switched off at 530s and an ELM of 50MJ is triggered at that time (indicated by a dashed line). From top to bottom: plasma energy, alpha heating, core and pedestal density and temperature are displayed. The time at which the H-L transition takes place is indicated by a vertical dashed line; the time at which the plasma energy decreases by e^{-1} from its value during the stationary burning plasma phase (which defines τ_W) is indicated by the intersection of the horizontal dashed line with the time trace of the plasma energy.
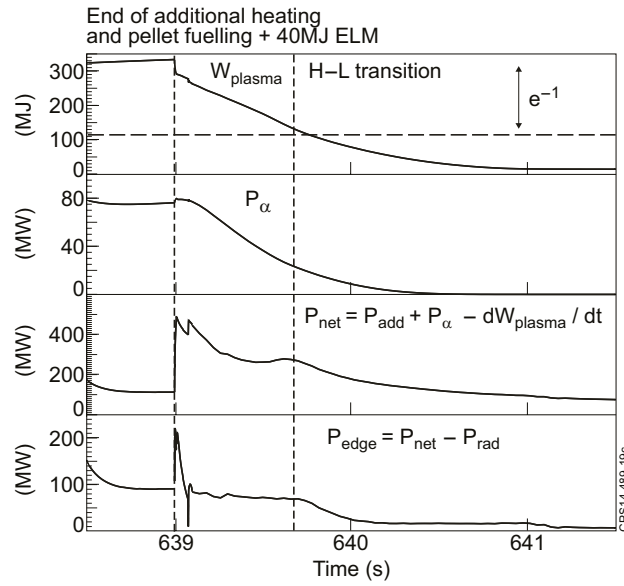
27

Figure 19: Modelling of the sudden termination of a $Q_{DT} = 10$ H-mode plasma in ITER when additional heating and pellet fuelling are switched off at 639s and an ELM of 40MJ is triggered at that time (indicated by a long-dashed line) which causes a W influx of $2\ 10^{19}$ W atoms. From top to bottom: plasma energy, alpha heating, net power ($P_{input} - dW_{plasma}/dt$, where $P_{input} = P_{add} + P_{ohmic} + P_\alpha$) and power crossing the separatrix (P_{edge}) are displayed. The time at which the H-L transition takes place is indicated by a vertical short-dashed line; the time at which the plasma energy decreases by e^{-1} from its value during the stationary burning plasma phase (which defines τ_W) is indicated by the intersection of the horizontal dashed line with the time trace of the plasma energy.